wet weight) was isolated as deep purple solid from methanol (mp 248-250 °C),[25] and **2** (24 mg, 0.012% wet weight) was isolated as a purple oil.

Acknowledgment. Partial research support was from NOAA, National Sea Grant College Program, Department of Commerce, Grant NA85AA-D-SG140, Project R/MP-41, through the California Sea Grant College Program. The U.S. Government is authorized to produce and distribute reprints for governmental purposes. Additional support was from NIH Grant CA47135-01A1. Fellowship support to W.D.I. included a Sea Grant Traineeship and a UC Institute of Marine Resources Dissertation Year fellowship. We thank Dr. C. Still for the MACROMODEL (V1.5) computer program, Dr. T. Wipke for the use of the Molecular Engineering Laboratory at UC, Santa Cruz, and NSF for a grant (DMB-8521802) to purchase the Evans and Sutherland (PS 330) graphics terminal. We are also grateful for assistance in sponge collection by Drs. T. Matthews, H. Chaney, and G. J. Bakus.

(25) All attempts to crystallize **1** did not yield X-ray quality crystals; however, long, thin branched needles were obtained.

Principal Values of Carbon-13 NMR Chemical Shift Tensors for a Collection of Substituted Benzenes

K. R. Morgan* and Roger H. Newman

Contribution from the Chemistry Division, DSIR, Private Bag, Petone, New Zealand.
Received December 23, 1988

Abstract: Principal values of 63 NMR chemical shift tensors were determined for atomic carbon atoms in 12 di-, tri-, and tetrasubstituted benzenes. The values were calculated from CP/MAS carbon-13 NMR spectra with the Herzfeld-Berger method. An empirical chemical shift additivity relationship was established for substitution by hydroxyl, methoxyl, aldehyde, carboxylic acid, and substituted alkyl functional groups. This relationship was successful in predicting principal values, usually within ±5 ppm.

Knowledge of spinning side-band (SSB) intensity patterns can be useful in any attempt at quanitative CP/MAS NMR, particularly if a high-field or medium-field magnet is involved. This is well illustrated by calculations for an aromatic CH group, based on typical chemical shift tensor (CST) data reviewed by Veeman[1] and graphs provided by Herzfeld and Berger.[2] For carbon-13 NMR at 50 MHz, it would be necessary to spin the sample at 12 kHz to confine 95% of the signal in the center band or at 20 kHz to confine 98% in the center band. Until these goals can be achieved in routine work, it would seem more reasonable to run spectra at more readily attainable spinning speeds and use correction factors to allow for signal strength lost in the side bands. This approach has been used, for example, in CP/MAS NMR experiments for quantitative determination of lignin in wood.[3]

Such applications of the Herzfeld-Berger SSB theory[2] depend on the availability of an adequate database for CST principal values. Recent reviews by Veeman[1] and Duncan[4] tabulate data for aromatic carbon in benzene and derivatives, with only a few examples of oxygen-substituted rings. We have now expanded the available data by determining CST principal values for 12 more substituted benzenes, all substituted by oxygen at 1 or more ring sites. We set out to generate a chemical shift additivity relationship so that we could predict CST principal values for generalized substitution patterns such as may be found in lignin or low rank coals.

A paper by Carter et al.,[5] published since this work was completed, has described similar substitutional effects for a series of three methoxyl benzenes. In this case, chemical shift tensors were determined by single-crystal studies.

Substituent chemical shift effects are most easily obtained from spectra of the monosubstituted benzene. This approach was not used in our solid-state NMR study because most of the substances are liquids at normal probe operating temperatures. We chose instead to use di-, tri-, and tetrasubstituted benzenes, followed by a regression analysis of the observed chemical shifts. All of the compounds in the collection contained at least one methoxyl group. The rotational motion of methoxyl groups provided an efficient proton spin-lattice relaxation mechanism, ensuring that reasonably short recovery delays could be used.

Scheme I

Compound	R_1	R_2	R_3	R_4
1	CO_2H	H	OCH_3	H
2	CO_2H	OCH_3	OH	H
3	CO_2H	OCH_3	OCH_3	H
4	CO_2H	OCH_3	OH	OCH_3
5	CHO	OCH_3	OH	H
6	CHO	OCH_3	OCH_3	H
7	CHO	OCH_3	OH	OCH_3
8	H	OCH_3	OH	OCH_3
9	H	OCH_3	OCH_3	OCH_3
10	CH_2OH	OCH_3	OH	H
11	$CH(CH_3)_2$	H	OH	H
12	$(CH_2)_3OH$	OCH_3	OH	H

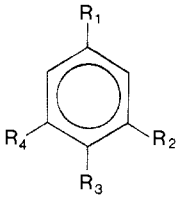

Several methods have been used to obtain CST principal values from ^{13}C NMR spectra of solids; these have been reviewed by Veeman.[1] We avoided the use of single crystals because of the difficulty involved in producing crystals of adequate size and because of the number of spectra required for a full description of the angular dependence of resonance frequencies. We also avoided simulation of spectra of static powders, because of the number of overlapping patterns in the spectra of our selected compounds and the consequent chances of errors. Even for a relatively simple aromatic compound such as xylene, the CST principal values measured from powder spectra[6] differed with a

(1) Veeman, W. S. *Prog. Nucl. Magn. Reson. Spectrosc.* **1984**, *16*, 193-235.
(2) Herzfeld, J.; Berger, A. E. *J. Chem. Phys.* **1980**, *73*, 6021-6030.
(3) Hemmingson, J. A.; Newman, R. H. *J. Wood Chem. Technol.* **1983**, *5*, 159-188.
(4) Duncan, T. M. *J. Phys. Chem. Ref. Data* **1987**, *16*, 125-151.
(5) Carter, C. M.; Facelli, J. C.; Alderman, D. W.; Grant, D. M.; Dalley, N. K.; Wilson, B. E. *J. Chem. Soc., Faraday Trans. 1* **1988**, *84*, 3673-3690.

0002-7863/90/1512-4$02.50/0

root-mean-square deviation of 11 ppm from those obtained in a single-crystal study.[7] We chose instead the Herzfield–Berger method[1] which involves graphical presentations of SSB patterns for dimensionless parameters combining CST principal values, the NMR frequency, and the MAS frequency. The method was originally tested on ^{31}P NMR spectra.[2] That work and subsequent publications[8,9] demonstrated good agreement between the results from ^{31}P NMR SSB patterns and the results from other methods. Typical CST anisotropies are not as large for ^{13}C nuclei, and the high-order SSB signals tend to be weaker and, therefore, less useful in graphical solutions. Nevertheless, the procedure has been used to determine CST principal values for ^{13}C in, e.g., polyacetylene,[10] quinol,[11] and retinal[12] derivatives.

Experimental Section

Substitution patterns for the 12 substituted benzenes are shown in Scheme I. Polycrystalline samples were packed in Kel-F rotors, and CP/MAS NMR spectra were obtained on a Varian XL-200 spectrometer operating at 50.3 MHz. Each 1-ms contact time was followed by 50 ms of data acquisition and a recovery delay of at least 3 times the proton spin–lattice relaxation time. Preliminary experiments showed that the spin–lattice relaxation time constants were all in the range 0.6–10.0 s. Chemical shifts were measured relative to TMS, with hexamethylbenzene used as a secondary reference.[13] A chemical shift of $\delta = 17.4$ ppm was used for the methyl signal of hexamethylbenzene.

Assignments were based on published solution NMR data.[14-16] Where confusion existed between close peaks from protonated and nonprotonated carbons, a spin-locking pulse sequence was used to suppress signals from the protonated carbon; the C-1 signal for veratic acid (**3**) was assigned on this basis.

Peak areas were obtained by cutting and weighing. Recorded spectra were repeated over a range of spinning frequencies between 1.0 and 2.4 kHz, so that at least one spectrum showed a sufficient number of first-order and/or second-order SSB signals for unambiguous use of Herzfeld–Berger graphs. Spinning frequencies were usually kept within ±10 Hz of the target frequency throughout each experiment, and spectra were rejected if broadening of the SSB signals indicated a drift of more than 1% during accumulation. The MAS probe used in this work allowed such stable, reproducible spinning frequencies that very few spectra were rejected.

Reliability of the method was tested by comparing chemical shift tensors for the carboxylic acid carbon of alanine determined by the Herzfeld–Berger method with those determined by single-crystal and powder methods. We also found that our results for 1,2.3-trimethoxybenzene were in good agreement with those of Carter et al.[5]

Solution NMR spectra were run on a Varian FT-80A spectrometer. The solvent was 90:10 (by volume) acetone-d_6:H_2O.

Discussion

Model compounds were included in the regression analysis only if all substituents were present in at least one other model compound. Therefore, compounds **10**, **11**, and **12** were not included in the regression analysis. The results for these 12 compounds are listed in Table I.

The resonances for C-2 and C-6 of **7**, C-3 and C-5 of **1**, and C-3 and C-5 of **11** were resolved in the CP/MAS NMR spectra, although in solution NMR experiments the pairs of signals collapse to singlets. The nonequivalence is attributed to conformational and possibly crystallographic effects and has been noted previously for anisic acid[17] (**1**). Splittings of the C-2 and C-5 resonances for **5** are attributed to the presence of at least two crystallographically nonequivalent molecules in the unit cell.

Our model for chemical shift additivity included five factors, namely ipso, ortho, meta, and para substituent effects plus two

Table I. Principal Values of Chemical Shift Tensors

compd	carbon	δ_{11}	δ_{22}	δ_{33}	δ_{av}	δ_{soln}
1	C-1	211	132	18	120.5	123.8
	C-2,6	233	154	8	131.8	132.4
	C-3	194	136	2	110.4	114.4
	C-4	248	178	70	165.4	164.2
	C-5	190	129	20	116.2	114.4
2	C-1	209	135	19	120.9	122.8
	C-2	*a*	*a*	*a*	111.5	113.6
	C-3	214	160	65	146.4	148.2
	C-4	229	159	64	150.8	152.1
	C-5	*a*	*a*	*a*	112.9	115.6
	C-6	218	137	14	123.2	124.8
3	C-1	*a*	*a*	*a*	122.1	123.8
	C-2	*a*	*a*	*a*	110.7	113.1
	C-3	224*[b]	160	65	149.3	149.6
	C-4	228	167	68	154.4	154.1
	C-5	*a*	*a*	*a*	110.7	111.6
	C-6	*a*	*a*	*a*	125.7	124.4
4	C-1	205	136	19	120.1	121.5
	C-2,6	176	126	10	104.3	108.1
	C-3,5	212	156	72	146.6	148.3
	C-4	202	153	58	137.8	141.5
5	C-1	*a*	*a*	*a*	128.6	130.5
	C-2	173*	142	0	104.7	111.1
	C-2′	174*	143	1	106.7	111.1
	C-3	*a*	*a*	*a*	148.0	149.1
	C-4	218	173	71*	154.0	153.8
	C-5	*a*	*a*	*a*	114.7	116.1
	C-5′	*a*	*a*	*a*	116.7	116.1
	C-6	*a*	*a*	*a*	128.6	127.1
6	C-2	*a*	*a*	*a*	130.4	130.9
	C-2	*a*	*a*	*a*	105.8	110.3
	C-3	213	167	67	149.1	150.5
	C-4	218	175	67	154.2	155.5
	C-5	*a*	*a*	*a*	107.4	111.8
	C-6	*a*	*a*	*a*	130.4	127.1
7	C-1	210	160	13	127.8	128.7
	C-3,5	213	163	69	148.0	149.1
	C-4	203*	165	59	142.8	143.3
	C-6	178	122	3	101.2	107.9
8	C-1	228	129	4*	120.2	124.5
	C-2,6	187	123	8	105.6	106.4
	C-3,5	209	164	72	148.4	154.4
	C-4	191	155	60	135.5	139.0
9	C-1	226	137	11	124.9	119.3
	C-2,6	184	125	8	105.7	106.5
	C-3,5	219*	1711	72	154.2	148.9
	C-4	179*	159	78*	138.6	136.8
10	C-1	223	165	15	134.7	
	C-3	218	157	71	149.2	
	C-4	221	151	66	146.0	
	C-6	215*	131	20*	122.2	
11	C-1	226	189*	15	143.3	
	C-2,6	223*	141*	23*	128.8	
	C-3,5	206*	130*	15	117.0	
	C-3′,5′	205*	128*	14	115.5	
	C-4	251	146	63	153.0	
12	C-1	234	151*	16	133.8	
	C-2	200	116*	16*	110.8	
	C-3	215	163	71	149.8	
	C-4	218	154	60	144.3	
	C-5	198	120*	32*	116.8	
	C-6	220*	129	26	124.8	

[a] Not determined because of overlapping signals. [b] * indicates predicted values differ by more than ±5 ppm for compounds **1–9** and by ±8 ppm for compounds **10–12**.

(6) Wemmer, D. E.; Pines, A.; Whitehurst, D. D. *Philos. Trans. R. Soc. London* **1981**, *A300*, 15–41.
(7) van Dongen Torman, J.; Veeman, W. S. *J. Chem. Phys.* **1978**, *68*, 3233–3235.
(8) Clayden, N. J.; Dobson, C. M.; Lian, L.-Y.; Smith, D. J. *J. Magn. Reson.* **1986**, *69*, 476–487.
(9) Griffiths, L.; Root, A.; Harris, R. K.; Chippendale, A. P.; Tromans, R. F. *J. Chem. Soc., Dalton Trans.* **1986**, 2247–2251.
(10) Mehring, M.; Weber, H.; Muller, W.; Wegner, G. *Solid State Commun.* **1983**, *45*, 1079–1082.
(11) Burgar, M. I. *J. Phys. Chem.* **1984**, *88*, 4929–4930.
(12) Harbison, G. S.; Mulder, P. P. J.; Pardoen, H.; Herzfeld, J.; Lugtenburg, J.; Griffin, R. D. *J. Am. Chem. Soc.* **1985**, *107*, 4809–4816.
(13) Earl, W. L.; VanderHart, D. L. *J. Magn. Reson.* **1982**, *48*, 35–54.
(14) Luedemann, H.-D.; Nimz, H. *Makromol. Chem.* **1974**, *175*, 2393–2407.
(15) Kringstad, K. P.; Morck, R. *Holzforschung* **1983**, *37*, 237–244.
(16) Scott, K. N. *J. Am. Chem. Soc.* **1972**, *94*, 8564–8568.
(17) Hays, G. R. *J. Chem. Soc., Perkin Trans. 2* **1983**, 1049–1052.

Table II. Best Fit Additivity Parameters

group	position	$\delta_{11}{}^k$	$\delta_{22}{}^k$	$\delta_{33}{}^k$	$\delta_{AV}{}^k$
CO_2H	ipso	−22 ± 4	6 ± 2	9 ± 3	−2.3
CO_2	ortho	−8 ± 3	6 ± 2	*a*	−0.7
CO_2H	meta	*a*	−5 ± 2	−4 ± 2	−3.0
CO_2	para	13 ± 3	*a*	*a*	4.3
CHO	ipso	−20 ± 6	30 ± 3	*a*	3.3
	ortho	−12 ± 3	*a*	−6 ± 3	−6.0
	para	7 ± 3	11 ± 2	*a*	6.0
OH	ipso	*a*	23 ± 2	55 ± 3	26.0
	ortho	−44 ± 4	−14 ± 2	15 ± 3	−14.3
	para	−7 ± 4	−21 ± 2	*a*	−9.3
OCH_3	ipso	*a*	30 ± 1	62 ± 3	30.3
	ortho	−44 ± 3	−7 ± 1	14 ± 3	−12.3
	meta	*a*	2 ± 1	*a*	1.2
	para	−7 ± 3	−15 ± 2	*a*	−7.3
X[b]	ipso	*a*	45	*a*	15.0
	meta	8	*a*	7	5.0
	para	*a*	−15	−6	−7.0
steric	S^a	21 ± 2		−15 ± 4	20
steric S^B	*a*	*a*	−15 ± 3	−50	

[a] Parameter removed to minimize the data. [b] Average for substituted alkyl groups i.e., X = CH_2OH, $CH(CH_3)_2$, $(CH_2)_3OH$.

steric effects or "crowding" effects. The first four factors are commonly used in additivity relationships.[18] One steric effect, S^A, is for oxygen-substituted carbons at adjacent ring sites. This effect was first employed by Woolfenden and Grant[19] to improve predictions for methylbenzenes and has been used more recently by Scott[16] for a series of hydroxyl- and methoxyl-substituted benzoic acids, some of which were included in the present study. The second effect used by Carter et al.[5] in their analysis, S^B, accounts for the fixed conformation of the methoxyl methyl group in the solid state and determines the steric repulsion between the methyl and an adjacent ortho hydrogen. This parameter was assigned on the basis of expected steric conformations and where a choice exists on the basis of the δ_{33} component as in the paper of Carter et al.[5]

Best fit parameters were sought for a relationship of the form

$$\delta_{ii} = K_{ii} + S^j q_{ii}{}^j + \sum G^k \delta_{ii}{}^k \qquad (1)$$

where the index i denotes each of the three principal axes of the CST, K_{ii} are constant terms, k is an index defining the type and position (i.e., ipso, ortho, meta, or para) of the substituent relative to the carbon atom of interest, $G^k = 1$ if the specified substituent is present at the specified position, $G^k = 0$ otherwise, and $\delta_{ii}{}^k$ are the substituent parameters to be determined.

The steric effect parameter S^j can be 0, 1, or 2 for j = A or B as explained above; $q_{ii}{}^j$ are then the parameters to be determined for these effects.

Substituent effects were determined with the MINITAB[20] routine REGRESS to perform a multiple regression calculation on the data of Table I combined with published results for solid benzene,[21] quinol,[10] and C-2 and C-5 of veratraldehyde.[22] Rather than include results from the analysis of Carter et al., we decided to carry out an independent analysis and compare the two sets of results. The parameter set was minimized by using the STEP REGRESS procedure of MINITAB to remove parameters that were only marginally significant.

Best fit parameters are given in Table II. The best fit values of K_{ii} were K_{11} = 238, K_{22} = 144, and K_{33} = 11 ppm, all close to the CST principal values for unsubstituted benzene,[21] i.e., 234, 146, and 9 ppm. Correlation coefficients of 97.7, 99.4, and 99.0 were obtained for δ_{11}, δ_{22}, and δ_{33} respectively. Most CST principal values were predicted by the model within ±5 ppm, although a few with larger differences are marked with asterisks in Table I.

The results for compounds **10**, **11**, and **12** were not included in the regression analysis because each of the three compounds contained a unique substituent. CST principal value increments were estimated for these three substituents by using eq 1 to allow for the effects of the other substituents. The results for the three substituents were then averaged and reported in Table II as best fit parameters for substitution by alkyl groups. These averaged best fit parameters give a fit with a root-mean-square deviation of 8 ppm from the CST principal values. Deviations larger than ±8 ppm are marked by asterisks beside the experimental data.

The effects of oxygen substitution are a positive increment for δ_{22} and δ_{33} for the ipso position and a negative increment for δ_{11} and δ_{22} for the ortho and (to a lesser extent) the para positions. The effects of substitution by carbon are almost entirely confined to δ_{11} and δ_{22}. The two cases are not clearly separated when all three principal values are averaged, as in solution NMR; e.g. the chemical shift for the carbon-substituted C-1 of **11** then lies within the range of chemical shifts for oxygen-substituted aromatic carbon in other compounds (Table I).

Substitution by carboxylic acid or aldehyde functional groups introduced chemical shift increments of only a few parts per million in the solution NMR spectra, but the best fit CST parameters of Table II show that some of these small changes are the sums of larger changes of opposing signs. A similar observation has been made in the case of substitution by methyl groups.[6]

Comparison of our methoxyl substitution effects with those of Carter et al. shows some major differences, but these are mostly confined to steric effects. For δ_{22} there is good agreement between the two results. However, with the addition of the steric factor, S^A, our own analysis gave very good agreement with the results of Carter et al.[5] for δ_{33} and to a lesser extent with δ_{11}. The correlation coefficient for δ_{11} is not nearly as high as for the other two principal components. This may be due to additional steric factors that have been neglected in our analysis. With the present limited size of our data set, it is not possible to consider fitting other steric factors. For similar reasons, it is not possible to separate out steric factors, S^A, for both methoxyl and hydroxyl substitution.

Interpretation of Results. In the case of benzene, the principal axes labeled 1–3 are aligned along the x, y, and z axes defined as directions radial, tangential, and perpendicular (respectively) relative to the ring. The directions are not so strictly confined by symmetry as in other cases, but single-crystal studies of polymethylbenzenes[23,24] have shown that the axes deviate only slightly from the directions defined above. Even in the more sterically crowded environment around the aromatic ring of pyromellitic acid,[25] deviations of only 5° have been reported. It appears likely that, for most of the compounds we studied, the principal axes are similarly close to the x, y, and z axes.

Chemical shielding is due to field-induced circulation of the surrounding electrons. The dominant effect for ^{13}C, the local paramagnetic effect, was shown by Ramsey[26] to be of the form

$$\delta_{jj} = K\sum_n (E_0 - E_n)\langle 0|L_j|n\rangle\langle n|2L_j/r^3|0\rangle$$

Here L is the j component of the angular momentum and acts as a rotation operator. It is, therefore, expected that if the field is parallel to a local symmetry axis, along a substituent bond, then the additivity effect on the adjacent carbon will be zero. Thus, for the ipso additivity effect, the δ_{11} (radial) component of the chemical shift tensor for an aromatic carbon should show only minimal changes while the δ_{22} and δ_{33} components should show the larger changes. Clearly this is so for the ipso additivity parameter for both methoxyl and hydroxyl substitutions which

(18) Ewing, D. F. *Org. Magn. Reson.* **1979**, *12*, 499–519.
(19) Woolfenden, W. R.; Grant, D. M. *J. Am. Chem. Soc.* **1966**, *88*, 1496–1502.
(20) Ryan, T. A., Jr. Computation Center, Pennsylvania State University, Philadelphia.
(21) Strub, H.; Beeler, A. J.; Grant, D. M.; Michl, J.; Cutts, P. W.; Zilm, K. W. *J. Am. Chem. Soc.* **1983**, *105*, 3333–3334.
(22) Terao, T.; Fujii, T.; Onodera, T.; Saika, A. *Chem. Phys. Lett.* **1984**, *107*, 145–148.
(23) Pausak, S.; Pines, A.; Waugh, J. S. *J. Chem. Phys.* **1973**, *59*, 591–595.
(24) Pausak, S.; Tegenfeldt, J.; Waugh, J. S. *J. Chem. Phys.* **1974**, *61*, 1338–1344.
(25) Tegenfeldt, J.; Feucht, H.; Ruschiztka, G.; Haeberlen, U. *J. Magn. Reson.* **1980**, *39*, 509–520.
(26) Ramsey, N. F. *Phys. Rev.* **1950**, *78*, 699–703.

have large δ_{22} and δ_{33} components but negligible δ_{11} component. The large steric effect that is observed for the ipso position with methoxyl and hydroxyl substitution then probably accounts for deviations of the substituent bond from the radial axis. If this factor is absent from the regression analysis, then an increase in the δ_{11} component was found and a lower correlation coefficient. Additional steric factors may account for the observed large δ_{11} ipso additivity factor with carboxyl and carbonyl substitution, but these were not considered because of the limited amount of data for these positions.

For carbon atoms ortho or para to an oxygen substitution site, the largest increments were observed on δ_{11} and δ_{22}. This can be explained by release of electrons from the oxygen atom to the π-orbitals of the ring. Additional electron density expands the carbon p_z orbitals, decreasing the $\langle r^{-3} \rangle$ factor and, therefore, weakening the paramagnetic contribution along the x and y axes. A similar effect has been reported by Strub et al.[21] for aromatic rings with five, six, or seven carbon atoms.

Substitution had little effect on the chemical shifts for the meta carbons, and this is consistent with charge-density alternation around the ring.

Conclusions

We have determined the principal values of the CST for aromatic carbons for a range of methoxyl- and hydroxyl-substituted benzene derivatives. With this large data set incorporated into a simple linear additivity model, the changes in the principal values of the CST with substitution can be predicted within a few parts per million.

Such uncertainties are small enough for the predicted CST principal values to be useful in quantitative CP/MAS NMR, through generation of correction factors to be applied to measurements of the center-band signal strength.

Registry No. 1, 100-09-4; **2**, 121-34-6; **3**, 93-07-2; **4**, 530-57-4; **5**, 121-33-5; **6**, 120-14-9; **7**, 134-96-3; **8**, 91-10-1; **9**, 634-36-6; **10**, 498-00-0; **11**, 99-89-8; **12**, 2305-13-7.

Intracrystalline Mass Transfer in Zeolites Monitored by Microscopic and Macroscopic Techniques

Christoph Förste, Jörg Kärger,* and Harry Pfeifer

Contribution from the Sektion Physik der Karl-Marx-Universität. Linnéstrasse 5. DDR-7010 Leipzig. German Democratic Republic. *Received January 3, 1989*

Abstract: Conventional ^{1}H NMR signal intensity measurements have been used to monitor macroscopically the kinetics of molecular exchange of deuterium-labeled molecules between the intracrystalline space of zeolite crystallites and the surrounding atmosphere. After reaching equilibrium, a pulsed-field-gradient experiment was performed within the same sample tube so that it became possible for the first time to compare results for the intracrystalline migration of adsorbed molecules derived from macroscopic (intensity) and microscopic (pulsed-field-gradient) measurements on identical samples. For benzene adsorbed on zeolite Na-X the intracrystalline diffusivities resulting from these two measuring techniques are found to be in satisfactory agreement. This result proves that molecular exchange between benzene adsorbed in the intracrystalline space of Na-X and the surrounding atmosphere is essentially controlled by intracrystalline mass transfer.

The advent of synthetic zeolites[1] has initiated a remarkable development in numerous branches of modern chemical technology.[2,3] It is basically the large, well-defined and modifiable intracrystalline pore volume of the zeolites that leads to their excellent properties as catalysts and molecular sieves. While, due to the combined application of X-ray scattering techniques,[4,5] high-resolution electron microscopy,[6] and magic angle spinning NMR,[7-9] a large variety of zeolite crystal structures are fairly well-known, for more than one decade the rate of mass transfer within the intracrystalline pore system has been the topic of controversial discussion.[10-17] This controversy has been brought about by the exciting result of the first NMR pulsed-field-gradient experiments[10,18] that in several cases the intracrystalline molecular mobilities in zeolites are by up to 5 orders of magnitude larger than previously determined on the basis of molecular uptake measurements.[19,20] A critical reconsideration of the uptake technique led to the conclusion that in several cases molecular uptake was limited by processes whose time constants previously

(1) Barrer, R. M. *Hydrothermal Chemistry of Zeolites*; Academic Press: London, 1982.
(2) Fijima, A., Ward, J. W., Eds. *New Developments in Zeolite Science and Technology*; Proceedings of the 7th International Zeolite Conference, Kodansha: Tokyo, 1986.
(3) Flank, W. H., Whyte, T. E., Eds. *Perspectives in Molecular Sieve Science*; ACS Symposium Series 368; American Chemical Society: Washington, DC, 1988.
(4) Bennett, J. M. Reference 3; pp 162-176.
(5) Hasha, D.; de Saldarriaga, L. S.: Saldarriaga, C.; Hathaway, P. E.: Cox, D. F.: Davis, M. E. *J. Am. Chem. Soc.* **1988**, *110*, 2127-2135.
(6) Thomas, J. M.; Millward. G. R.; Ramdas, S.; Bursill. L. A.; Audier, M. *Faraday Discuss. Chem. Soc.* **1981**, *No. 72*, 345-352.
(7) Lippmaa, E.; Mägi, H.; Samson, A.; Engelhardt, G.; Grimmer, A. R. *J. Am. Chem. Soc.* **1980**, *102*, 4889-4893.
(8) Strobl, H.; Fyfe. C. A.; Kokotailo, G. T.; Pasztor, C. T.; Bibby, D. M. *J. Am. Chem. Soc.* **1988**, *109*, 4733-4734.
(9) Pfeifer, H.; Freude, D.; Hunger, M. *Zeolites* **1985**, *5*, 274-286.
(10) Kärger, J.; Caro, J. *J. Chem. Soc., Faraday Trans. 1* **1977**, *73*, 1363-1376.
(11) Ruthven, D. M. *ACS Symp. Ser.* **1977**, *40*, 320-334.
(12) Gelbin, D.; Fiedler, K. *AIChE J.* **1980**, *26*, 510-513.
(13) Goddard. M.; Ruthven. D. M. Reference 2; pp 467-473.
(14) Bülow, M.; Öhlmann, G. In *New Developments in Zeolite Science and Technology—Discussion*: Tominaga, H., Ed.; Japan Association of Zeolites: Tokyo, 1986; p 68.
(15) Ruthven, D. M.: Eic, M. Reference 3; pp 362-375.
(16) Kärger, J.; Pfeifer, H. Reference 3; pp 376-396.
(17) Eic, M.; Goddard. M.; Ruthven. D. M. *Zeolites* **1988**, *8*, 327-331.
(18) Kärger, J.; Pfeifer, H.; Heink. W. *Adv. Magn. Reson.* **1988**, *12*, 1-89.
(19) Ruthven, D. M. *Principles of Adsorption and Adsorption Processes*: Wiley: New York, 1984.
(20) Barrer, R. M. *Zeolites and Clay Minerals as Adsorbents and Catalysts*: Academic Press: London, 1978.

0002-7863/90/1512-7$02.50/0